Backstepping Control for Induction Motors with Input and Output Constraints

Tung Lam Nguyen
Department of Industrial Automation
University of Science and Technology
Hanoi, Vietnam
lam.nguyentung@hust.edu.vn

Thanh Ha Vo
Department of Electrical Engineering
University of Transportation and
Communications, Hanoi, Vietnam
vothanhha.ktd@utc.edu.vn

Nam Duong Le
Department of Electrical Engineering
Quy Nhon University
Quy Nhon, Vietnam
lenamduong@qnu.edu.vn

Abstract−**In practice, the applied control voltage for an induction motor drive system fed by a voltage source inverter has a limit depending on the DC bus capacity. In certain operations such as accelerating, the motor might require an excessively high voltage value that the DC bus cannot supply. This paper presents a control solution for the bounded control input problem of the induction motor system by flexibly combining a hyperbolic tangent function in a backstepping control design procedure. In addition, the Barrier Lyapunov function is also employed to force speed tracking error in a defined value. The closed-loop system stability is proven, and the proposed control is verified through numerical simulations.**

Keywords-backstepping; Barrier Lyapunov funtion; induction motor; FOC

I. INTRODUCTION

Induction motors have been serving as a major workforce in various industrial applications [1, 2] due to their robustness and ease of maintenance. Despite the fact that technologies used in induction motor drive systems are well-established, the drive system still draws control researchers' attention due to its complicated dynamical properties [3, 5]. In the two most common induction motor drive control techniques, Flux Oriented Control (FOC) [6] based schemes are widely used when compared to Direct Torque Control (DTC) structure [7]. FOC renders the induction motor as a direct current motor in terms of decoupling torque producing and flux forming process. There have been many attempts to control the induction motor based on FOC, from classical PID control [2] to advance nonlinear strategies including model predictive control [8], sliding mode control [9], fuzzy-neural approach [10], and genetic algorithm [11]. Thanks to its systematic design and the ability to cope with system nonlinearities, backstepping method is intensively used in the induction motor drive. Authors in [12] successfully employed backstepping integrated with a high-gain observer for stabilizing the motor drive without information on the rotor speed, flux, and load torque. In order to compensate system uncertainties, backstepping was combined with a recurrent neural network to enhance tracking performance in induction servo systems [13]. A similar approach can be found in [14] where a radial basis function neural network was used. The proposed control guarantees system stability and bounded signals. Exploiting the

robustness of sliding mode control, authors in [15] designed a backstepping sliding mode control for dealing with lumped uncertainties in linear induction motor drives. The effectiveness of the proposed control is verified numerically and experimentally. In [16], adaptive backstepping control supported by a fuzzy system for integral action was developed for a linear induction motor. Simulation study showed the control ability to cope with parameter variations and load disturbances. In the quest of compensating system mechanical parameters such as unknown viscous coefficient and load torque, an adaptive backstepping algorithm was designed in [17]. Other applications of backstepping control in induction motor drive can be seen in [18, 19].

The aforementioned researches mainly focus on ways to improve the dynamical responses of the induction motor drive closed-loop system regardless the limitations of the control inputs. It is clearly that in certain circumstances, the motor might require exceeded voltage value that the DC bus cannot supply. If the required voltage is not satisfied, it results in system performance degradation. In this paper, a method is introduced to tackle the problem by manipulating backstepping control with the assistance of a virtual control defined through a hyperbolic tangent function for limiting the control input in a specified value determined by the capacity of the DC bus. In addition, the paper also integrates Barrier Lyapunov function in the design steps in order to force the speed tracking error falling in a desired range.

II. MATHEMATICAL MODEL FORMULATION

The mathemathetical model of the induction motor is well defined, for more detailed derivation please refer to [20]. The induction motor model in the *d-q* reference frame is obtained as in (1) where: $\sigma = 1 - \dfrac{L_m^2}{L_s L_r}$ is the leakage factor, $T_s = \dfrac{L_s}{R_s}$ the stator time constant, $T_r = \dfrac{L_r}{R_r}$ the rotor time constant, $k_r = \dfrac{L_m}{L_r}$, $r_\sigma = R_s + R_r k_r^2$, $T_\sigma' = \dfrac{\sigma L_\sigma}{r_\sigma}$, $\omega_s = \omega + \dfrac{L_m}{T_r}\dfrac{i_{sd}}{\psi_{rd}}$ the slip estimation, ω is the mechanical rotor speed, z_p is the number of pole pairs, J is the rotor and load lumped inertia, T_L the load torque, ψ_{rd}

Corresponding author: Tung Lam Nguyen

the rotor flux, and L_m, L_r, L_s: mutual, rotor, and stator inductance.

$$\begin{cases} \dfrac{di_{sd}}{dt} = -\left(\dfrac{1}{\sigma T_s} + \dfrac{1-\sigma}{\sigma T_r}\right)i_{sd} + \omega_s i_{sq} + \dfrac{1-\sigma}{\sigma T_r}\psi'_{rd} + \dfrac{1}{\sigma L_s}u_{sd} \\[2mm] \dfrac{di_{sq}}{dt} = -\omega_s i_{sd} - \left(\dfrac{1}{\sigma T_s} + \dfrac{1-\sigma}{\sigma T_r}\right)i_{sq} - \dfrac{1-\sigma}{\sigma}\omega\psi'_{rd} \\[2mm] \qquad + \dfrac{1-\sigma}{\sigma T_r}\psi'_{rq} + \dfrac{1}{\sigma L_s}u_{sq} \\[2mm] \dfrac{d\psi'_{rd}}{dt} = \dfrac{1}{T_r}i_{sd} - \dfrac{1}{T_r}\psi'_{rd} + (\omega_s - \omega)\psi'_{rq} \\[2mm] m_M = \dfrac{3}{2}z_p\dfrac{L_m^2}{T_r}\psi'_{rd}i_{sq} = -\dfrac{3}{2}z_p(1-\sigma)L_s\psi'_{rd}i_{sq} \end{cases} \quad (1)$$

The first two equations characterize motor current dynamics. The last two equations denote motor flux forming process and equation of motion. It can be observed that the induction motor given in (1) is a coupled and nonlinear system. The block diagram representation of the induction motor is given in Figure 1.
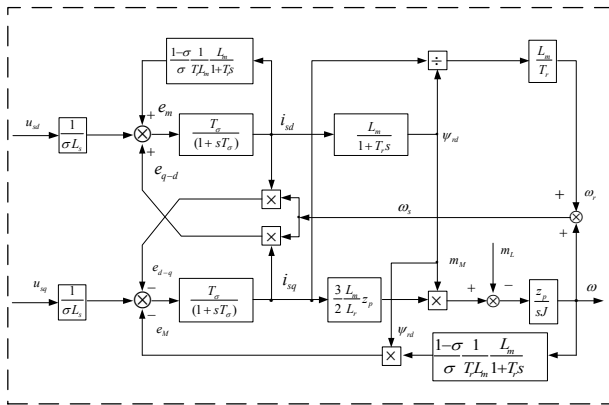

Fig. 1.   Structure of the induction motor in *dq*-coordinates.

III. BACKSTEPPING CONTROLLER DESIGN WITH CONTROL INPUT AND OUTPUT CONSTRAINS

A. Magnetic Flux Control Design

The control objective is to drive the motor magnetic flux to a desired value in such a way that the tracking error stays in a predefined range. In order to achieve this objective, the tracking error is defined as follows:

$$z_1 = x_1 - \varphi'_{rdref} \quad (2)$$

and a Lyapunov candidate function is:

$$V_1 = \frac{1}{2}\log\frac{k_b^2}{k_b^2 - z_{1d}^2} \quad (3)$$

Taking the time derivative of V_1 gives:

$$\dot{V}_1 = \frac{z_{1d}(x_2 - \dot{q}_d)}{k_b^2 - z_{1d}^2} \quad (4)$$

At this point, x_2 is considered as a control input, the error between x_2 and the desired control value is defined as:

$$z_2 = x_2 - \alpha_1 \quad (5)$$

where a_1 is the virtual control. Substituting (5) into (4) gives:

$$\dot{V}_1 = \frac{z_{1d}(z_2 + a_1 - \dot{q}_d)}{k_b^2 - z_{1d}^2} \quad (6)$$

Equation (6) suggests that the virtual control can be selected as:

$$a_1 = c_1 z_{1d} + x_2 + \frac{\dot{q}_d - \dot{x}_1}{(k_b^2 - z_{1d}^2)} \quad (7)$$

The virtual control renders $\dot{V}_1$ as:

$$\dot{V}_1 = -c_1 z_{1d}^2 + z_{1d}z_2 \quad (8)$$

To deal with the coupling term $z_1 z_2$ and force z_2 to zero, we propose a Lyapunov candidate function as:

$$V_2 = \frac{1}{2}z_{2d}^2 + V_1 \quad (9)$$

The derivative of V_2 will have the following form:

$$V_2 = -c_1 z_{1d}^2 + z_{1d}z_{2d} + z_{2d}\dot{z}_{2d} \quad (10)$$

Taking the derivative of (5) we have:

$$\dot{z}_2 = -c_1\dot{z}_1 - \frac{(\ddot{q}_d - \ddot{x}_1)(k_{b1}^2 - z_{1d}^2) - 2z_{1d}^2\dot{z}_1}{(k_{k1}^2 - z_{1d}^2)^2} \quad (11)$$

Substituting the first and second equations (10) to (11) results in:

$$\dot{z}_2 = \frac{1}{T_r\left(k_{b1}^2 - z_{1d}^2\right)}\left(-\frac{1}{T_\sigma}x_2 + \omega_s x_1 + \frac{1-\sigma}{\sigma T_\sigma}x_1 + \frac{1}{\sigma T_\sigma}u_{sd}\right)$$
$$- \frac{1}{T_r\left(k_{b1}^2 - z_{1d}^2\right)}\left(\frac{1}{T_\sigma}x_2 - \frac{1}{T_r}x_1\right) + c_1\left(\frac{1}{T_r}x_2 - \frac{1}{T_r}x_1 - \dot{q}_d\right) \quad (12)$$
$$+ \frac{2z_{1d}^2}{\left(k_{b1}^2 - z_{1d}^2\right)^2}\left(\frac{1}{T_r}x_2 - \frac{1}{T_r}x_1 - \dot{q}_d\right) - \ddot{q}_d$$

From (10) and (12) the control signal can be achieved guaranteeing x_1 converges to *dq* with the dynamical error confined in a range defined by k_b. Another control objective is to specify the control input subject to a limitation. It is necessary to consider input constrains in the control design since the applied voltage is supplied from an inverter whose output voltage is practicallye limited. Toward this end, the limitation of the output voltage is described as a tangent function.

$$u_{sd} \equiv g(\upsilon) = u_M \tanh\left(\frac{\upsilon}{u_M}\right) \quad (13)$$

where u_M is the control limit. The design of u_{sd} is passed to the construction of ϑ. Equation (13) results in:

$$\dot{g}(\upsilon) = \frac{\partial g(\upsilon)}{\partial \upsilon}\dot{\upsilon} \quad (14)$$

The control design of u_{sd} is subject to $u_{sd} \le u_M$ is a shift to a task of finding a virtual signal U_1 defined by:

$$\dot{\upsilon} = \frac{\partial g(g)^{-1}}{\partial \upsilon}U_1 \quad (15)$$

To proceed we define:

$$z_3 = u_{sd} - \alpha_2 \equiv g(\upsilon) - \alpha_2 \quad (16)$$

From (12) and (16) the virtual control a_2 can be selected as:

$$
\begin{aligned}
\alpha_2 &= -\sigma L_\sigma T_r (k_{b1}^2 - z_1^2)(z_1 + \frac{1}{T_r(k_{b1}^2 - z_1^2)}(-\frac{x_2}{T_\sigma} + \omega_s x_1 \\
&+ \frac{1-\sigma}{\sigma T_r}x_1 - \frac{1}{T_r(k_{b1}^2 - z_1^2)}(\frac{1}{T_r}x_2 - \frac{1}{T_r}x_1) \\
&+ c_1(\frac{1}{T_r}x_2 - \frac{1}{T_r}x_1 - \dot{q}_d) + \frac{2z_1^2}{(k_{b1}^2 - z_1^2)^2}(\frac{1}{T_r}x_2 - \frac{1}{T_r}x_1 - \dot{q}_d) \\
&- \ddot{q}_d + c_2 z_2)
\end{aligned}
\quad (17)
$$

Virtual control a_2 renders $\dot{V}_2$ as:

$$\dot{V}_2 = -c_1 z_1^2 - c_2 z_2^2 + \frac{1}{(k_{b1}^2 - z_1^2)T_r \sigma L_s}Z_2 Z_3 \quad (18)$$

In order to remove the coupling term related to $z_2 z_3$ and drive $g(\upsilon)$ to track a_2, a Lyapunov candidate function is proposed as follows:

$$V_3 = \frac{1}{2}z_3^2 + V_2 \quad (19)$$

The derivative of (19) yields:

$$\dot{V}_3 = -c_1 z_1^2 - c_2 z_2^2 + \frac{1}{(k_{b1}^2 - z_1^2)T_r \sigma L_s}z_2 z_3 + z_3 \dot{z}_3 \quad (20)$$

Taking the derivative of (16) and substituting the result into (20), we can finally get the virtual control that guarantees bounded control input as:

$$U_1 = -\frac{1}{(k_{b1}^2 - z_1^2)T_r \sigma L_s}z_2 + \dot{a}_2 - c_3 z_3 \quad (21)$$

Substituting the proposed control into (20) gives:

$$\dot{V}_3 = -c_1 z_1^2 - c_2 z_1^2 - c_3 z_3^2 \le 0 \quad (22)$$

and the design process for magnetic flux is completed.

B. Speed Control Design

The speed control design with input and output constrains is carried out in the same manner as in the previous section. For the sake of abstract presentation, control design steps are summarized in this section as follows:

$$t_1 = x_3 - \dot{\omega}_{ref} \quad (23)$$

$$\beta_1 = -d_1 t_1 + x_4 - \frac{\dot{x}_2 - \dot{\omega}_{ref}}{k_{b1}^2 - t_1^2} \quad (24)$$

$$t_2 = x_4 - \beta_1 \quad (25)$$

$$
\begin{aligned}
\beta_2 &= -\frac{J\sigma L_s(k_{b1}^2 - t_1^2)}{k_m x_1}(\frac{k_m x_1}{J(k_{b1}^2 - t_1^2)}(-\omega_s x_2 - \frac{x_4}{T_\sigma} - \frac{1-\sigma}{\sigma}\omega x_1) \\
&+ \frac{k_m x_4}{J(k_{b1}^2 - t_1^2)}(\frac{1}{T_r}x_2 - \frac{1}{T_r}x_1) - \frac{\dot{\omega}_{ref}}{(k_{b1}^2 - t_1^2)} + t_1 \\
&+ \frac{2t_1^2}{(k_{b1}^2 - t_1^2)^2}(\frac{k_m x_1 x_4}{J} - \dot{\omega}_{ref}) + d_1(\frac{k_m x_1 x_4}{J} - \dot{\omega}_{ref}) + d_2 t_2)
\end{aligned}
\quad (26)
$$

$$t_3 = u_{sq} - \beta_2 = g(\upsilon) - \beta_2 \quad (27)$$

$$U_2 = -\frac{k_m x_1}{(k_{b1}^2 - t_1^2)J\sigma L_s}t_2 + \dot{\beta}_2 - d_3 t_3 \quad (28)$$

where β_1, β_2 are virtual controls and t_1, t_2, t_3 are the backstepping design errors in each step. The control signal guaranteeing bounded input and output is U_2.

IV. SIMULATION RESULTS

A. Settings

Simulations were conducted on an IM machine with the structure control for induction motor shown in Figure 2. The space vector modulation is used for the inverter part. R_ψ, R_ω, and R_I, are flux, speed, and dq-current controllers, respectively. Simulation parameters are given in Table I. In the simulation, two control schemes were implemented: conventional and input-output embedded backstepping controls.

TABLE I.   SIMULATION PARAMETERS

Rated power	P_{nom}	2.2kW
Speed motor	n_{nom}	2880prm
Rated phase current	I_{nom}	4.7A$_{RMS}$
Number of pole pairs	z_p	1
Rotor resistance	R_r	0.42Ω
Stator resistance	R_s	0.37Ω
Rotor inductance	L_r	34.25mH
Stator inductance	L_s	34.41mH
Mutual inductance	L_m	33.1mH
Total inertia	J	0.001kgm^2

B. Simulation Procedure

At $t=0s$, magnetic current is created and at $t=2s$ the system speeds up to 1200rpm. In the simulation scenario, a sudden torque with rated value of 1.5Nm is applied on the motor shaft. The results of the simulation of stator current and speed controllers using conventional backstepping control method and backstepping with control input and output constrains are shown in Figures 3-8 where (a) represents the response of conventional backstepping and (b) represents the backstepping with input and output constraints. The proposed backstepping controller is applied to the induction motor. The coefficients are chosen as: c_1=1000, c_2=1000, c_3=5150, c_4=1000, d_1=500, d_2=500, d_3=1000, and d_4=500.
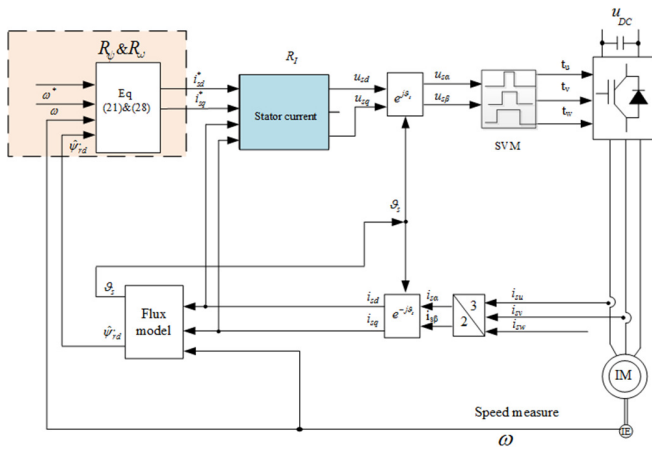
Fig. 2.   Backstepping control with output and input contraints.

In the simulation result, the control signal constraint is selected as:

$$U_s = \sqrt{u_{sd}^2 + u_{sq}^2} \le 160V \quad (29)$$

Constraints on *dq* are determined according to rectangular approximation:

$$u_{sq}^{max} = \alpha \frac{V_{dc}}{\sqrt{3}} \quad \text{and} \quad u_{sd}^{max} = \sqrt{1-\alpha^2} \frac{V_{dc}}{\sqrt{3}} \quad (30)$$

where V_{dq}=300V and *a*=0.8. This condition implies that control inputs must satisfy:

$$|u_{sq}| \le u_{sq}^{max} \quad \text{and} \quad |u_{sd}| \le u_{sd}^{max} \quad (31)$$

The designed controller can also limit the system's output through the value k_b. This helps us to control the overshoot of the system. In the simulation, we set the value k_b=0.1.
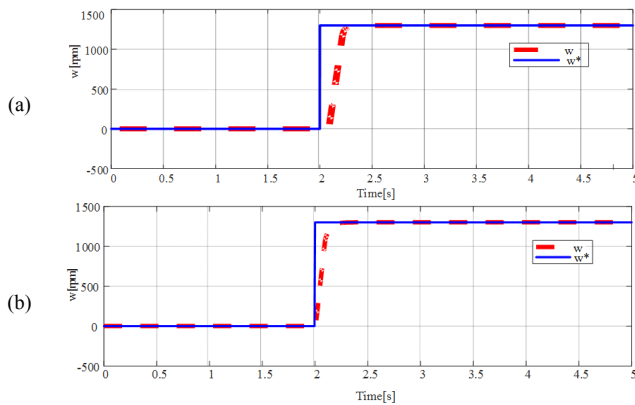

Fig. 3.   Speed response.

For the system controlled by the conventional backstepping method, we set the dc bus voltage to $V_{dc} = 300V$. This implies that there is no hard limit applied in this case. On the contrary, the dc bus voltage is restricted to 160V when the induction motor drive system is regulated by backstepping control with input and output constraints. In both cases, simulation results

show that the two approaches provide good tracking performance with fast response time as can be seen in Figure 3.
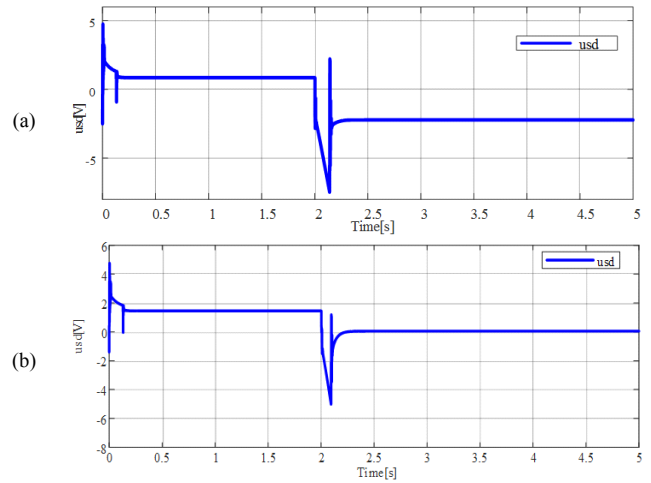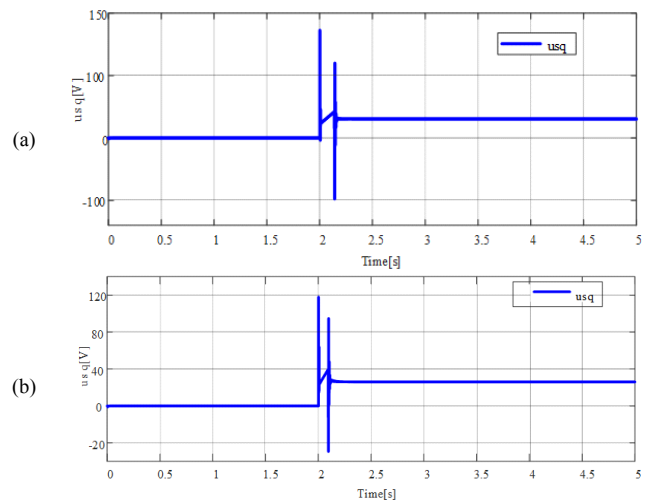

Fig. 4.   Voltage response u_{sd}.
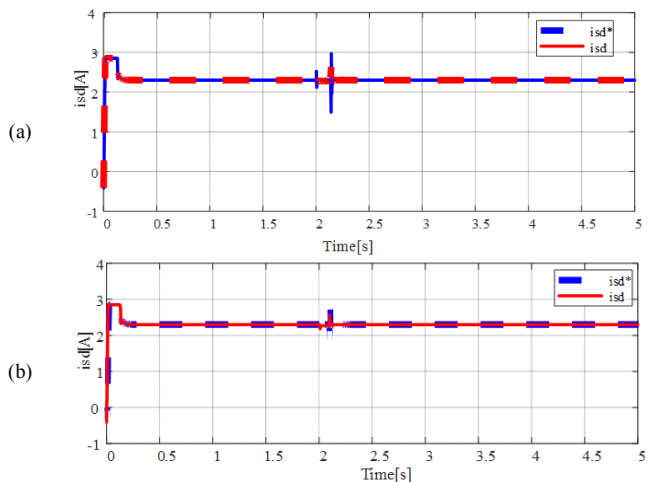

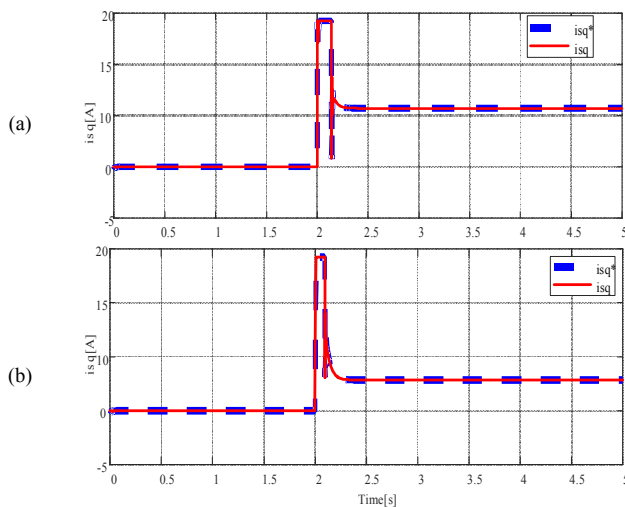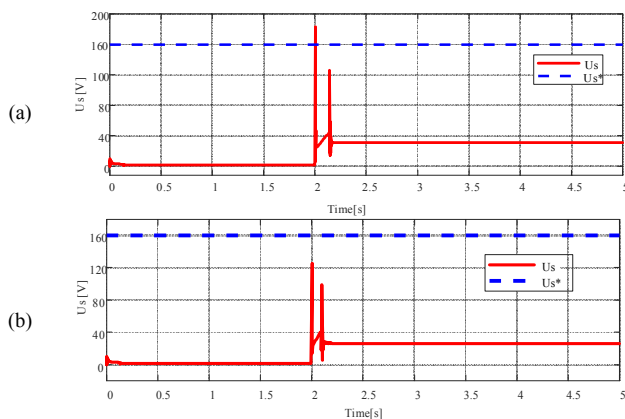Fig. 5.   Voltage response u_{sq}.

Fig. 6.   Stator current responses i_{sd}.

Fig. 7.   Stator current responses i_{sq}.

Fig. 8.   Voltage U_s response.

It is noted that at 2s the motor accelerates to 1200rpm. This speeding action requires a considerably large quadrature current and voltage (Figures 4(a), 5(a), 6(a), and 7(a)), resulting in U_s reaching 180V in the case of the conventional method as shown in Figure 8(a). Meanwhile, due to the fact that the control inputs are tied to 160V, the U_s measured values when the backstepping with input and output limitation action is suppressed well below 120V (Figures 4-8(b)). The results show technical meaning when the system requires large control input when fast accelerating or deaccelerating in the face of limited dc bus capacity. The speed tracking also indicates that the overshoot remains in the bounded set specified by $k_b = 0.1$. We see that the controller designed by this method helps the drive system respond well in accordance with the set values. However, the disadvantage of this method is that it is difficult to select the optimal coefficients for the controller, the design process of calculating control signals requires many derivative steps leading to a large volume of calculations.

V. CONCLUSION

The paper proposes a control mechanism backboned by backstepping control to avoid voltage saturation in induction motor drive systems. The hyperbolic tangent is embedded in the control design to deal with the voltage saturation problem. This approach differs from other works where either torque producing or flux forming voltage is sacrificed when the input voltage enters the saturation zone. The simulation results show that the control can suppress the control input voltage in the prescribed domain while maintaining the tracking error due to the help of the barrier Lyapunov function. In future research, we aim at deploying the proposed control in an experimental rig.

REFERENCES

[1] X. Shi, H. Li, and J. Huang, "A Practical Scheme for Induction Motor Modelling and Speed Control," *International Journal of Control and Automation*, vol. 7, pp. 113–124, Apr. 2014, doi: 10.14257/ijca.2014.7.4.11.

[2] T. M. Chikouche, A. Mezouar, T. Terras, and S. Hadjeri, "Variable Gain PI Controller Design For Speed Control of a Doubly Fed Induction Motor Using State-Space Nonlinear Approach," *Engineering, Technology & Applied Science Research*, vol. 3, no. 3, pp. 433–439, Jun. 2013.

[3] "A robust sensorless output feedback controller of the induction motor drives: new design and experimental validation," *International Journal of Control*, vol. 83, no. 3, pp. 484–497, doi: 10.1080/00207170903193474.

[4] V. T. Ha, V. H. Phuong, N. T. Lam, and N. P. Quang, "A dead-beat current controller based wind turbine emulator," in *2017 International Conference on System Science and Engineering (ICSSE)*, Ho Chi Minh City, Vietnam, Jul. 2017, pp. 169–174, doi: 10.1109/ICSSE.2017.8030859.

[5] V. T. Ha, N. T. Lam, V. T. Ha, and V. Q. Vinh, "Advanced control structures for induction motors with ideal current loop response using field oriented control," *International Journal of Power Electronics and Drive Systems (IJPEDS)*, vol. 10, no. 4, pp. 1758–1771, Dec. 2019.

[6] J. Zhang *et al.*, "Integrated design of speed sensorless control algorithms for induction motors," in *2015 34th Chinese Control Conference (CCC)*, Jul. 2015, pp. 8678–8684, doi: 10.1109/ChiCC.2015.7261011.

[7] M. K. Sahu, A. K. Panda, and B. P. Panigrahi, "Direct Torque Control for Three-Level Neutral Point Clamped Inverter-Fed Induction Motor Drive," *Engineering, Technology & Applied Science Research*, vol. 2, no. 2, pp. 201–208, Apr. 2012.

[8] S. M. Kazraji and M. B. B. Sharifian, "Model predictive control of linear induction motor drive," in *IECON 2017 - 43rd Annual Conference of the IEEE Industrial Electronics Society*, Oct. 2017, pp. 3736–3739, doi: 10.1109/IECON.2017.8216635.

[9] C. Regaya, A. Zaafouri, and A. Chaari, "A New Sliding Mode Speed Observer of Electric Motor Drive Based on Fuzzy-Logic," *Acta Polytechnica Hungarica*, vol. 11, pp. 219–232, Feb. 2014, doi: 10.12700/APH.11.03.2014.03.14.

[10] M. Denai and S. Attia, "Fuzzy and neural control of an induction motor," *International Journal of Applied Mathematics and Computer Science*, vol. 12, pp. 221–233, Jan. 2002.

[11] M. Chebre, A. Meroufel, and Y. Bendaha, "Speed Control of Induction Motor Using Genetic Algorithm-based PI Controller," *Acta Polytechnica Hungarica*, vol. 8, no. 6, pp. 141–153, Jan. 2011.

[12] I. Haj Brahim, S. Hajji, and A. Chaari, "Backstepping Controller Design using a High Gain Observer for Induction Motor," *International Journal of Computer Applications*, vol. 23, no. 3, pp. 1-6, Jun. 2011, doi: 10.5120/2873-3730.

[13] C. M. Lin and C. F. Hsu, "Recurrent-neural-network-based adaptive-backstepping control for induction servomotors," *IEEE Transactions on Industrial Electronics*, vol. 52, no. 6, pp. 1677–1684, Dec. 2005, doi: 10.1109/TIE.2005.858704.

[14] J. Yu, Y. Ma, B. Chen, H. Yu, and S. Pan, "Adaptive neural position tracking control for induction motors via back stepping," *International Journal of Innovative Computing, Information and Control*, vol. 7, no. 7, pp. 4503–4516, Jul. 2011.

[15] F.-J. Lin, P.-H. Shen, and S.-P. Hsu, "Adaptive backstepping sliding mode control for linear induction motor drive," *IEE Proceedings - Electric Power Applications*, vol. 149, no. 3, pp. 184–194, May 2002, doi: 10.1049/ip-epa:20020138.

[16] I. K. Bousserhane, A. Hazzab, R. Mostefa, B. Mazari, and M. Kamli, "Mover position control of linear induction motor drive using adaptive backstepping controller with integral action," *Tamkang Journal of Science and Engineering*, vol. 12, pp. 17–28, Mar. 2009.

[17] H. T. Lee, "Adaptive PC-based backstepping position control of induction motor," *International Journal of Power Electronics*, vol. 3, no. 2, p. 156, 2011, doi: 10.1504/IJPELEC.2011.038891.

[18] M. Moutchou, A. Abbou, and H. Mahmoudi, "MRAS-based sensorless speed backstepping control for induction machine, using a flux sliding mode observer," *Turkish Journal of Electrical Engineering and Computer Sciences*, vol. 23, pp. 187–200, Jan. 2015, doi: 10.3906/elk-1208-50.

[19] M. Morawiec, "Dynamic variables limitation for backstepping control of induction machine and voltage source converter," *Archives of Electrical Engineering*, vol. 61, no. 3, pp. 389–410, 2012, doi: 10.2478/v10171-012-0031-1.

[20] N. P. Quang and J.-A. Dittrich, *Vector Control of Three-Phase AC Machines: System Development in the Practice*, 2nd ed. Berlin Heidelberg: Springer-Verlag, 2015.